

# Energy Minimization for UAV-Enabled Covert Offloading MEC Systems

Yi Zhou, Zheng Ma, Pingzhi Fan, Azzam Al-nahari, Phee Lep Yeoh, Branka Vucetic and Yonghui Li

**Abstract**—In this work, a covert offloading framework is established for unmanned aerial vehicle (UAV) system. Specifically, one UAV-enabled mobile edge computing (MEC) server is deployed to assist the offloading for multiple ground users, while the offloading behavior might be exposed and detected due to the existence of a malicious warden. To enhance the covertness, each user splits a part of its power to transmit jamming signal, and the relationship between users' power split ratio and the warden's minimum detection error probability (DEP) is investigated. Then, an efficient energy minimization algorithm is designed by optimizing users' power split, computing resource allocation and deployment of the UAV-MEC server jointly, subject to specific covertness, power and transmission rate constraints. Finally, simulation results are provided to demonstrate the effectiveness of our covert offloading design.

**Index Terms**—UAV, MEC, jamming, covert offloading.

## I. INTRODUCTION

Unmanned aerial vehicles (UAVs), which can be deployed on-demand to provide seamless and prompt communication services, are strong technical supporters for sixth-generation (6G) wireless network [1], [2]. In [3], a multi-UAV communication system was devised with the objective of achieving substantial throughput gains. In this system, UAVs function as aerial base stations, facilitating connectivity and communication services from the skies. Furthermore, [4] employed stochastic geometry to conduct a statistical analysis of both single- and multi-swarm UAV configurations, with a focus on maximizing coverage probability using millimeter wave (mmWave) propagation techniques.

Y. Zhou is with the Information Coding & Transmission (ICT) Key Laboratory of Sichuan Province, Southwest Jiaotong University, Chengdu 610031, China, and also with School of Computer Science, Brunel University London, London, UB8 3PH, UK (e-mail: yizhou@swjtu.edu.cn).

Z. Ma and P. Fan are with the Information Coding & Transmission (ICT) Key Laboratory of Sichuan Province, Southwest Jiaotong University, Chengdu 610031, China. (e-mail: zma@home.swjtu.edu.cn; pzf@swjtu.edu.cn).

Azzam Al-nahari is with the Department of Information and Communications Engineering, Aalto University, 02150 Espoo, Finland, and also with the Department of Electrical Engineering, Ibb University, Ibb, Yemen (e-mail: azzamyn@gmail.com).

P. L. Yeoh is with the School of Science, Technology and Engineering, University of the Sunshine Coast, Australia (e-mail: pyeoh@usc.edu.au).

B. Vucetic and Y. Li are with the School of Electrical and Information Engineering, University of Sydney, NSW 2006, Australia (e-mail: branka.vucetic@sydney.edu.au; yonghui.li@sydney.edu.au).

This work was supported in part by the National Key R&D Program of China under Grant 2023YFB2603500, in part by the National Natural Science Foundation of China under Grant 62271419, Grant 62301462, Grant 62361136810, and Grant U2268201, in part by UKRI Postdoc Guarantee project S-ISAC [grant number EP/Z002435/1] and EU MSCA Postdoctoral Fellowships [grant number 101154926].

In addition to communication functionalities, computing plays a significant role in the development of 6G networks [5]. Integrating computing resources onto UAV provides new opportunities to address the scarcity of computation services in remote areas, facilitated by the fast and flexible deployment capability of UAVs [6], [7]. In [8], to support the computational services in the Internet of Things (IoT), a collaborative UAV-aided edge computing system was introduced, employing centralized and distributed frameworks. Moreover, in [9], the latency and energy performance of a multi-UAV-aided MEC system was discussed by employing deep reinforcement learning (DRL) scheme.

However, the broadcast openness of UAV ground-to-air (G2A) propagation channel may lead to the easy detection of offloading behavior by malicious wardens [10]. This could potentially expose privacy information, including location and transmission status, and increasing the risk of ongoing attacks [11], [12]. Thus, guaranteeing the covertness and security of UAV communications is crucial [13], [14]. In [15], an energy-efficient covert communication strategy was designed for UAV-aided backscatter communication by leveraging noise uncertainty. In [16], a covert UAV-enabled intelligent reflection surface (IRS) system was proposed where the covertness is achieved by introducing the uncertainty of IRS phase shifting.

While existing works on UAV communications, such as [12], [15], [16], have addressed covertness, they primarily focused on communication functionalities without considering computing, and cannot be implemented in UAV-MEC system. Although MEC-related measurements such as latency and energy were minimized in UAV-MEC systems, the designed frameworks in [8], [9] remain vulnerable to malicious attacks, thus compromising the security performance. To the best of our knowledge, no prior work has been devoted to protect the UAV-MEC system from being detected by a malicious warden, thus strongly motivating this work.

To fill this gap, in this paper, a covert UAV-enabled offloading MEC framework is developed where one UAV-MEC server is deployed to assist the offloading for multiple ground users, in the presence of a malicious warden who attempts to detect the offloading behavior. From the covertness perspective, each user splits part of its power to send jamming signal and confuse the warden under channel uncertainty. We envision that such a covert offloading design can be implemented to support IoT applications in remote areas, such as data collection in power grids, environmental monitoring,

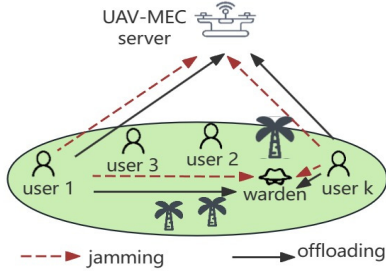


Fig. 1. A covert UAV-MEC system.

and green agriculture. The main contributions of this paper are summarized as follows.

- A covert offloading framework is proposed for UAV communications with power split on multiple ground users to send communication and jamming signals respectively, in the presence of a warden who detects the offloading of all ground users. The relationship between the covertness measurement and users' power split ratio is studied.
- An efficient energy minimization algorithm is designed for the UAV-MEC server subject to covertness, power and transmission rate constraints by optimizing the users' power split ratio, computing resource allocation and deployment of UAV-MEC server jointly.
- Simulation results are provided to show the effectiveness of our design. Moreover, the fundamental trade-off between energy consumption and covertness is revealed.

## II. SYSTEM MODEL AND PROBLEM FORMULATION

As shown in Fig. 1, a covert UAV-MEC system is established where  $K$  ground users with computing-intensive missions need to offload their tasks to the UAV-MEC server, in the presence of a malicious warden who launches detection attacks to confirm the offloading status of all users. To assist the offloading to be carried out covertly and securely, each user splits part of its power to send jamming signal and confuse the warden. Denote the amount of task generated by all ground users as  $D = \{D_1, D_2, \dots, D_K\}$ . Each user offloads its task to the UAV-MEC server one by one via time-division multiple access (TDMA), as shown in Fig. 2.

### A. Communication Model

Define the horizontal locations of user  $k$  and warden as  $\mathbf{r}_k = (x_k, y_k)^T, \forall k \in \mathcal{K}$  and  $\mathbf{r}_w = (x_w, y_w)^T$ , respectively. The UAV-MEC server hovering at an altitude of  $H$  m is deployed with horizontal position of  $\mathbf{r}_u = (x_u, y_u)^T$ . Consider that the G2A channels experience line-of-sight (LoS) and non line-of-sight (NLoS) propagation, where the LoS probability that depends on the elevation angle is given by [17]

$$P_{L,k} = \frac{1}{1 + a \exp(-b[\theta_k - a])}, \quad (1)$$

with  $a$  and  $b$  being the environmental constants. Moreover,  $\theta_k = \frac{180}{\pi} \tan^{-1} \left( \frac{H}{\|\mathbf{r}_u - \mathbf{r}_k\|} \right)$  is the elevation angle between user  $k$  and the UAV-MEC server. Denote  $h_{L,k}$  as the path-loss

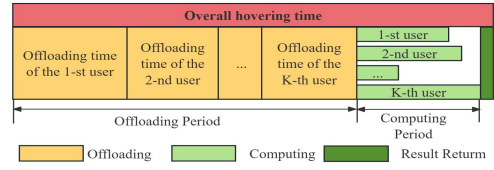


Fig. 2. Time schedule.

between user  $k$  and UAV-MEC server for LoS propagation, which is given by

$$h_{L,k} = \frac{\beta_0}{(\|\mathbf{r}_u - \mathbf{r}_k\|^2 + H^2)^{\frac{\alpha_L}{2}}}, \quad (2)$$

where  $\beta_0$  represents the G2A channel gain at a reference distance of one meter and  $\alpha_L$  is the path-loss exponent for LoS link. As the NLoS link suffers from additional attenuation, thus, the achievable rate for the NLoS link is much lower than that can be achieved via LoS link [18]. Moreover, as the users and UAV-MEC server are within a same coalition to against the warden, thus, the jamming signal from the users can thus be perfectly canceled at the UAV-MEC server via successive interference cancellation (SIC) technical. As such, the achievable rate between user  $k$  and UAV-MEC server is approximated by its LoS part, and can be given by

$$R_k \approx P_{L,k} B \log_2 \left( 1 + \frac{p_k^c h_{L,k}}{\sigma_u^2} \right), \quad (3)$$

where  $p_k^c$  is the transmission power at user  $k$  to offload tasks. Moreover,  $\sigma_u^2$  denotes the noise power at the UAV-MEC server and  $B$  is the pre-allocated bandwidth.

For terrestrial communications, a Rayleigh fading channel is adopted due to the obstacles and blockages. The channel gain of user  $k$ -warden link is given by

$$h_{k,w} = \frac{\beta_1 g_k}{\|\mathbf{r}_k - \mathbf{r}_w\|^\alpha} = c_k g_k, \quad (4)$$

where  $c_k = \frac{\beta_1}{\|\mathbf{r}_k - \mathbf{r}_w\|^\alpha}$ ,  $\alpha$  is the path-loss exponent for ground communications and  $\beta_1$  represents the terrestrial channel gain at a reference distance of one meter. Moreover,  $g_k$  follows an exponential distribution with mean value of one, i.e.,  $f_G(g_k) = \exp(-g_k)$ .

### B. Computing Model

In this work, we consider that each user offloads all of its tasks to the UAV-MEC server for computing. As shown in Fig. 2, once the task from all users have been uploaded successfully, the UAV-MEC server allocates its computing resource to compute the tasks for each user simultaneously. When user  $k$  is associated, the time consumed for offloading  $D_k$  bits of data is given by

$$t_{o,k} = \frac{D_k}{R_k}, \forall k. \quad (5)$$

Moreover, the time consumed for computing the tasks of user  $k$  is given by

$$t_{c,k} = \frac{D_k F}{f_k}, \forall k, \quad (6)$$

where  $F$  is the number of central processing unit (CPU) cycles that will be used to compute one bit of data. Here, the downlink delay for result return is ignored due to the small data size of the result [19]. In addition,  $f_k$  represents the computing resource provided by the UAV-MEC server to compute  $D_k$ , where the sum of which should be bounded by the maximum budget  $f_{max}$ , i.e.,  $\sum_{k=1}^K f_k \leq f_{max}$ .

### C. Energy Model

From UAV's perspective, energy is mainly consumed for two parts. One part is for hovering, and the other part is for computing. Specifically, as shown in Fig. 2, the UAV-MEC server needs to hover in the air during the period of  $t_h = \sum_{k=1}^K t_{o,k} + \max(t_{c,k})$  with a hovering power of  $p_h = (3^{-3/4} + 3^{1/4})b_1^{1/4}b_2^{3/4}$ , where  $b_1$  and  $b_2$  are environmental constants. Thus, the hovering energy is given by

$$E_h = t_h p_h = \left( \sum_{k=1}^K \frac{D_k}{R_k} + \max\left(\frac{D_k F}{f_k}\right) \right) p_h. \quad (7)$$

Moreover, when UAV computes the tasks for the  $k$ -th user, as the power for computing is  $\nu f_k^3$ , thus, the corresponding computing energy to process the tasks for user  $k$  is given by

$$E_k = \nu f_k^3 \times \frac{D_k F}{f_k} = \nu f_k^2 D_k F, \quad (8)$$

where  $\nu$  is a coefficient related to the power in UAV-MEC server. Thus, the overall energy consumption at the UAV is given by

$$E = \left( \sum_{k=1}^K \frac{D_k}{R_k} + \max\left(\frac{D_k F}{f_k}\right) \right) p_h + \sum_{k=1}^K D_k F \nu f_k^2. \quad (9)$$

### D. Covertiness Performance

We consider that the warden judges the offloading behavior based on the detected power for each offloading. If user  $k$  is associated, the corresponding binary hypothesis test can be formulated as

$$P_k = \begin{cases} H_0 : p_k^j h_{k,w} + \sigma_w^2 \\ H_1 : (p_k^j + p_k^c) h_{k,w} + \sigma_w^2, \end{cases} \quad (10)$$

where  $p_k^j$  is the power for sending the jamming signal at user  $k$ , and  $\sigma_w^2$  is the noise power at warden. The null hypothesis  $H_0$  implies that user  $k$  is not offloading data while the alternative hypothesis  $H_1$  indicates that user  $k$  is offloading data to the UAV-MEC server. Moreover, the statistic of this test is  $P_k \stackrel{D_1}{\geq} \tau$ , where  $\tau$  is the corresponding detection threshold. In addition,  $D_0$  and  $D_1$  are the decisions in favor of  $H_0$  and  $H_1$ , respectively.

1) *False Alarm Probability (FAP)*: FAP depicts the probability that the warden detects the offloading behavior of user  $k$  when  $H_0$  occurs, and can be given by

$$P_{FA,k} = Pr(D_1|H_0) = Pr(p_k^j c_k g_k \geq \tau - \sigma_w^2) = \begin{cases} \exp\left(-\frac{\tau - \sigma_w^2}{p_k^j c_k}\right), & \text{if } \tau \geq \sigma_w^2 \\ 1, & \text{if } \tau \leq \sigma_w^2, \end{cases} \quad (11)$$

where  $Pr(\cdot)$  represents the occurrence probability of the event.

2) *Miss Detection Probability (MDP)*: In contrast, MDP depicts the probability that warden does not detect the offloading behavior of user  $k$  when  $H_1$  happens, thus can be expressed as

$$P_{MD,k} = Pr(D_0|H_1) = Pr((p_k^j + p_k^c) c_k g_k \leq \tau - \sigma_w^2) = \begin{cases} 1 - \exp\left(-\frac{\tau - \sigma_w^2}{(p_k^j + p_k^c) c_k}\right), & \text{if } \tau \geq \sigma_w^2 \\ 0, & \text{if } \tau \leq \sigma_w^2. \end{cases} \quad (12)$$

3) *Minimum Detection Error Probability (DEP)*: When  $H_0$  and  $H_1$  occur with equal probability, the DEP, i.e.,  $\epsilon_k = P_{FA,k} + P_{MD,k}$ , can be expressed as

$$\epsilon_k = \begin{cases} 1 + \exp\left(\frac{\sigma_w^2 - \tau}{p_k^j c_k}\right) - \exp\left(\frac{\sigma_w^2 - \tau}{(p_k^j + p_k^c) c_k}\right), & \text{if } \tau \geq \sigma_w^2 \\ 1, & \text{if } \tau \leq \sigma_w^2. \end{cases} \quad (13)$$

From warden's perspective, the lower the DEP, the better the detection accuracy. Thus, it would like to intelligently select an optimal detection threshold, to achieve the minimum DEP. Next, we focus on the case when  $\tau \geq \sigma_w^2$  and investigate the minimum DEP,  $\epsilon_{k,min}$ , in the following lemma.

**Lemma 1.** The minimum DEP is given by

$$\epsilon_{k,min} = 1 + \exp\left(-\frac{\ln(1 + o_k)}{o_k(1 + o_k)^{-1}}\right) - \exp\left(-\frac{\ln(1 + o_k)}{o_k}\right), \quad (14)$$

where  $o_k = p_k^c/p_k^j$  is defined as user  $k$ 's covert power split ratio.

**Proof.** To show this, by taking the first-order derivative of  $\epsilon_k$  with respect to  $\tau$ , we have

$$\frac{\partial \epsilon_k}{\partial \tau} = \frac{\exp\left(-\frac{\tau - \sigma_w^2}{(p_k^j + p_k^c) c_k}\right)}{(p_k^j + p_k^c) c_k} - \frac{\exp\left(-\frac{\tau - \sigma_w^2}{p_k^j c_k}\right)}{p_k^j c_k}. \quad (15)$$

By solving (15), it can be seen that  $\frac{\partial \epsilon_k}{\partial \tau} \leq 0$  when  $\tau \leq \tau^*$ , while  $\frac{\partial \epsilon_k}{\partial \tau} \geq 0$  when  $\tau \geq \tau^*$ , where  $\tau^*$  is the optimal detection threshold that satisfies  $\frac{\partial \epsilon_k}{\partial \tau} = 0$ , which can be expressed as

$$\tau^* = \frac{\ln(1 + o_k)(p_k^j + p_k^c) c_k p_k^j}{p_k^c}. \quad (16)$$

By taking  $\tau^*$  into Eq. (13), Lemma 1 is proved.  $\square$

**Remark 1.** The minimum DEP  $\epsilon_{k,min}$  is a decreasing function in terms of user  $k$ 's covert power split ratio  $o_k = p_k^c/p_k^j$ .

**Proof.** To show this, by taking the first-order derivative of  $\epsilon_{k,min}$  in terms of  $o_k$ , we have

$$\frac{\partial \epsilon_{k,min}}{\partial o_k} = \frac{(1 + o_k)^{-\frac{1}{o_k}}}{(o_k)^2} \ln(1 + o_k) \left(-\frac{o_k}{1 + o_k}\right) \leq 0. \quad (17)$$

Thus, Remark 1 is proved.  $\square$

**Remark 2.** The minimum DEP  $\epsilon_{k,min}$  is independent of warden's location  $\mathbf{r}_w$ .

As we can see from (14),  $\epsilon_{k,min}$  only relies on the power split ratio  $o_k$  and is independent of warden's location. Since the warden would like to hide in somewhere to launch attack, its location information is usually unknown to users. Thus, the proposed covert UAV-MEC framework that is independent of warden's location is attractive in practical scenarios.

### E. Problem Formulation

In this work, aimed to minimize the energy consumption at the UAV-MEC server, an optimization problem is formulated subject to covert offloading, transmission rate and power constraints, by optimizing users' power split  $\{\mathbf{p}^j, \mathbf{p}^c\}$ , UAV deployment  $\mathbf{r}_u$ , and UAV computing resource allocation  $\mathbf{f}$  jointly. Thus, the optimization problem can be formulated as

$$\begin{aligned} & \underset{\mathbf{p}^j, \mathbf{p}^c, \mathbf{f}, \mathbf{r}_u, T_c}{\text{minimize}} \quad \left( \sum_{k=1}^K \frac{D_k}{R_k} + T_c \right) p_h + \sum_{k=1}^K D_k F \nu f_k^2 & (18a) \\ & \text{s.t. } \epsilon_{k,min} \geq 1 - \kappa, \forall k & (18b) \\ & R_k \geq R_0, \forall k & (18c) \\ & T_c \geq \frac{D_k F}{f_k}, \forall k & (18d) \\ & p_k^j + p_k^c \leq p_{k,max}, \forall k & (18e) \\ & \sum_{k=1}^K f_k \leq f_{max} & (18f) \\ & x_{min} \leq x_u \leq x_{max}, y_{min} \leq y_u \leq y_{max}, & (18g) \end{aligned}$$

where  $T_c$  corresponds to the maximum computing time among all  $K$  users. Constraints (18b) and (18c) ensure that the covertness and transmission rate requirements are satisfied for each user's offloading, respectively. Constraint (18e) implies that the power consumption at each user should not exceed the budget. Moreover, (18f) and (18g) are the constraints of overall computing resource and feasible range for deployment of UAV-MEC server, respectively.

### III. ENERGY MINIMIZATION ALGORITHM FOR COVERT UAV-MEC SYSTEM

In this section, an efficient solution is designed to solve Problem (18) via monotonicity and convexity analysis, as well as successive convex approximation (SCA) method.

#### A. Computing Resource Optimization

First, since the computing resource variable  $\mathbf{f}$  only makes impact to the computing energy and one part of the hovering energy without coupling with other variables, by removing the constant terms, the computing resource allocation problem can be equivalently transformed as

$$\underset{\mathbf{f}, T_c}{\text{minimize}} \quad p_h T_c + \sum_{k=1}^K D_k F \nu f_k^2 \quad (19a)$$

$$\text{s.t. } \sum_{k=1}^K f_k \leq f_{max}, T_c \geq \frac{D_k F}{f_k}, \forall k. \quad (19b)$$

It can be noticed that Problem (19) is convex, which can be solve efficiently via standard optimization tool, such as CVX.

#### B. Optimal Power Split at Users

Next, as users' power split only affects another part of hovering energy, by removing constant terms, the power split problem can be formulated as

$$\underset{\mathbf{p}^j, \mathbf{p}^c}{\text{minimize}} \quad \sum_{k=1}^K \frac{p_h D_k}{R_k} \quad (20a)$$

$$\text{s.t. } \epsilon_{k,min} \geq 1 - \kappa, \forall k, \quad (20b)$$

$$R_k \geq R_0, \forall k \quad (20c)$$

$$p_k^j + p_k^c \leq p_{k,max}, \forall k. \quad (20d)$$

According to Remark 1, on the one hand, we see that  $\epsilon_{k,min}$  decreases with increasing user  $k$ 's covert power split ratio  $o_k$ . On the other hand, increasing  $p_k^c$ , which corresponds to increasing  $o_k$ , is beneficial to enhance  $R_k$  and minimize the objective function. With above monotonic characteristics, to minimize  $\sum_{k=1}^K p_h D_k / R_k$  subject to a given  $\epsilon_{k,min}$  constraint, the optimal  $o_k^*$  can be obtained by meeting constraint (20b) exactly with equality, resulting in

$$o_k^* = \{o_k | \epsilon_{k,min}(o_k^*) = 1 - \kappa\}, \quad (21)$$

which can be found via bisection search method. Next, by rewriting  $p_k^j = p_k^c / o_k^*$ , (20d) can be re-expressed as

$$\frac{p_k^c}{o_k^*} + p_k^c \leq p_{k,max}, \forall k. \quad (22)$$

As  $R_k$  is an increasing function with respect to  $p_k^c$ , to minimize  $\sum_{k=1}^K \frac{p_h D_k}{R_k}$ , (22) should be met with equality, and the optimal powers are given by

$$p_k^{c*} = \frac{o_k^* p_{k,max}}{1 + o_k^*}, p_k^{j*} = \frac{p_{k,max}}{1 + o_k^*}. \quad (23)$$

We note that  $p_k^{c*}$  and  $p_k^{j*}$  only rely on the optimal power split ratio  $o_k^*$ , power budget, and covertness requirement, and they are independent of UAV deployment. Moreover, since the optimal power split is designed to maximize  $R_k$ , thus, this optimization is feasible only if (20c) is satisfied with optimal  $p_k^{c*}$ .

#### C. UAV Deployment Optimization

Then, by introducing four sets of auxiliary variables  $\{\chi, \omega, \iota, \psi\}$  and removing constant terms, the UAV deployment can be obtained by solving

$$\underset{\mathbf{r}_u, \chi, \omega, \iota, \psi}{\text{minimize}} \quad \sum_{k=1}^K \frac{p_h D_k}{B \chi_k} \quad (24a)$$

$$\text{s.t. } \underbrace{\frac{1}{\iota_k} \log_2 \left( 1 + \frac{s_k}{\omega_k} \right)}_{\mathcal{W}_k} \geq \frac{R_0}{B}, \forall k \quad (24b)$$

$$x_{min} \leq x_u \leq x_{max}, y_{min} \leq y_u \leq y_{max} \quad (24c)$$

$$\chi_k \leq \mathcal{W}_k, \forall k \quad (24d)$$

$$\omega_k \geq (\|\mathbf{r}_u - \mathbf{r}_k\|^2 + H^2)^{\frac{\alpha L}{2}}, \forall k \quad (24e)$$

$$\iota_k \geq 1 + a \exp(-b[\psi_k - a]) \quad (24f)$$

$$\psi_k \leq \frac{180}{\pi} \tan^{-1} \left( \frac{H}{\|\mathbf{r}_u - \mathbf{r}_k\|} \right), \quad (24g)$$

where  $s_k = \beta_0 p_k^c / \sigma_u^2$ . To proceed, it can be verified that  $\frac{1}{x} \log_2 \left(1 + \frac{1}{y}\right)$  is jointly convex in terms of  $x$  and  $y$  [18], and  $\tan^{-1}(1/z)$  is convex in terms of  $z$ .

As such, we observe that the non-convexity of Problem (24) arises from constraints (24b), (24d), and (24g). To tackle the non-convexity, we consider to approximate these constraints via SCA based on the first-order Taylor expansion as follows.

$$(24b) \rightarrow \frac{R_0}{B} \leq \mathcal{W}_k^{lb}, \forall k, \quad (25)$$

where  $\mathcal{W}_k^{lb}$  represents the lower bound of  $\mathcal{W}_k$  and is given by

$$\mathcal{W}_k^{lb} = \frac{1}{\iota_k[n]} \log_2 \left(1 + \frac{s_k}{\omega_k[n]}\right) - \frac{\iota_k - \iota_k[n]}{(\iota_k[n])^2} \log_2 \left(1 + \frac{s_k}{\omega_k[n]}\right) - \frac{s_k(\omega_k - \omega_k[n])}{\iota_k[n](s_k \omega_k[n] + (\omega_k[n])^2) \ln 2}, \forall k, \quad (26)$$

with  $\iota_k[n]$  and  $\omega_k[n]$  being the values of  $\iota_k$  and  $\omega_k$  in the  $n$ -th iteration, respectively. Similarly, (24d) can be approximated as

$$(24d) \rightarrow \chi_k \leq \mathcal{W}_k^{lb}, \forall k. \quad (27)$$

In addition, constraint (24g) can be approximated as

$$(24g) \rightarrow \psi_k \leq \frac{180}{\pi} \tan^{-1} \left( \frac{H}{\|\mathbf{r}_u[n] - \mathbf{r}_k\|} \right) - \frac{180}{\pi} \frac{H(\|\mathbf{r}_u - \mathbf{r}_k\| - \|\mathbf{r}_u[n] - \mathbf{r}_k\|)}{\|\mathbf{r}_u[n] - \mathbf{r}_k\|^2 + H^2}, \forall k, \quad (28)$$

where  $\mathbf{r}_u[n]$  is the value of  $\mathbf{r}_u$  in the  $n$ -th iteration.

With above transformation, the UAV deployment can be obtained by solving

$$\begin{aligned} & \underset{\mathbf{r}_u, \chi, \omega, \iota, \psi}{\text{minimize}} \quad \sum_{k=1}^K \frac{p_k D_k}{B \chi_k} \\ & \text{s.t.} \quad (24c), (24e), (24f), (25), (27), (28). \end{aligned} \quad (29a)$$

Now that Problem (29) is convex, it can thus be solved via standard optimization software, i.e., CVX.

#### D. Overall Algorithm

We summarize the main steps of our proposed solution in Algorithm 1, where computing resource allocation, users' optimal power split and UAV deployment are solved.

#### Algorithm 1 Proposed Energy Minimization Algorithm for Covert UAV-MEC Systems.

- 1: Initialization: Deploy the UAV at centroid among all users. Set  $p_k^c = 0.5$  W,  $p_k^j = 2$  W,  $f_k = f_{max}/K, \forall k$ .
- 2: Update computing resource allocation of UAV-MEC server  $\mathbf{f}$  by solving (19);
- 3: Update users' power allocation  $\mathbf{p}^c, \mathbf{p}^j$  based on (21) and (23), respectively;
- 4: **repeat**
- 5:   Update UAV deployment  $\mathbf{r}_u$  by solving Problem (29);
- 6: **until** convergence

#### IV. SIMULATION RESULTS

In this section, simulation results are presented to demonstrate the performance of our proposed energy minimization solution for covert UAV-MEC systems. We consider that

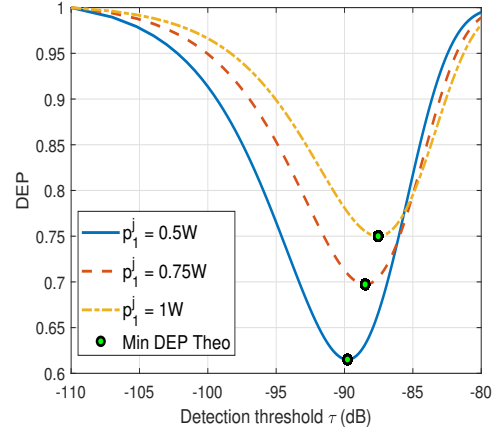


Fig. 3. DEP versus detection threshold.

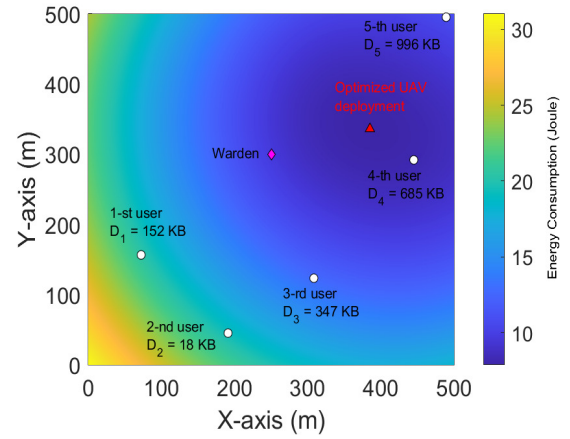


Fig. 4. Colormap of energy consumption with different UAV locations.

5 users need to offload their tasks which follow uniform distributions  $D_k \sim \mathcal{U}(0.1, 1)$  MB to the UAV-MEC server. As shown in Fig. 4, all users are randomly distributed within the range of  $[500 \text{ m}, 500 \text{ m}]$  with the power budgets that follow  $p_{k,max} \sim \mathcal{U}[3, 5]$  W. The warden is located at  $[250.45 \text{ m}, 300.24 \text{ m}]$ . Moreover, we set  $B = 1$  MHz,  $\kappa = 0.2$ ,  $F = 500$  cycles/bit,  $\beta_0 = \beta_1 = 10^{-3}$ ,  $\sigma_u^2 = \sigma_w^2 = -110$  dB,  $\alpha = 2.5$ ,  $f_{max} = 10$  GHz,  $H = 100$  m,  $R_0 = 0.5$  Mbit/s,  $\alpha_L = 2.2$ ,  $a = 9.61$ ,  $b = 0.16$ ,  $\nu = 10^{-27}$ ,  $b_1 = 0.002$ ,  $b_2 = 70.698$  [20].

In Fig. 3, the relationship between DEP and detection threshold  $\tau$  is plotted with different jamming powers of the 1-st user. We observe that the theoretical results for the minimum DEP that are obtained via Eq. (14), i.e., green dots as shown in Fig. 3, match the simulation results well, thus verifying the correctness of our derived theoretical expression. Moreover, we see that the larger the jamming power, the higher the DEP. This phenomenon can be understood since the uncertainty of warden's received power increases with a higher jamming power, resulting in a high probability that the warden makes an incorrect decision.

In Fig. 4, we plot the colormap of energy consumption



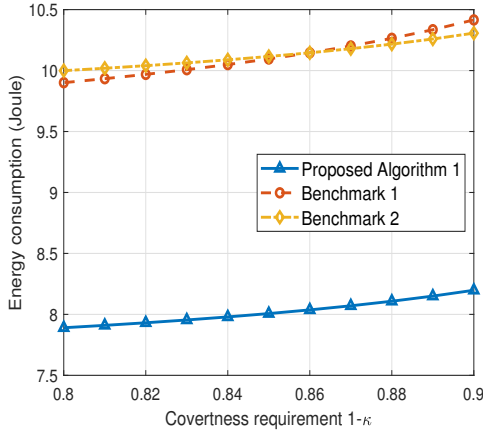


Fig. 5. Comparison with benchmark schemes.

with different UAV locations. Specifically, the locations of users and warden are represented by the white circles and purple diamond, respectively. We observe that our optimized UAV deployment, which is shown as the red triangle, achieves a low energy consumption of 7.89 Joule, thus verifying the effectiveness of our UAV deployment optimization.

To further demonstrate the superiority of our proposed solution, in the simulation, we compare our Algorithm 1 with the following two benchmark schemes.

- Benchmark 1: In this scheme, the UAV is hovering in the centroid among all users, and the users' power split and UAV computing resource are optimized via Algorithm 1.
- Benchmark 2: In this scheme, the users' power split and UAV deployment are obtained by Algorithm 1, while the UAV assigns its computing resource for executing the data of each user equally, i.e.,  $f_k = f_{max}/K, \forall k$ .

In Fig. 5, we compare our proposed Algorithm 1 with benchmark schemes on energy consumption over a wide range of covertness requirements. Several interesting observations can be found according to Fig. 5. First, we observe that with a more strict covertness requirement, i.e., a higher value of  $1-\kappa$ , the consumed energy increases at the UAV-MEC server, revealing that there exists a fundamental trade-off between covertness and energy consumption. This is because when the covertness is more challenging to achieve, according to Remark 1, a lower covert power split ratio  $o_k = p_k^c/p_k^j$  is expected, resulting in a reduced transmission rate  $R_k$  and increased energy consumption. Moreover, it can be seen that our proposed Algorithm 1 contributes to the lowest energy consumption when compared to benchmark solutions, indicating the importance of our joint design.

## V. CONCLUSIONS

In this paper, a UAV-aided covert offloading framework was developed with power split at users to send communication and jamming signals, respectively. Specifically, the relationship between covertness measurements and users' power split ratio was investigated theoretically. Moreover, an effective energy minimization algorithm was designed. Finally, simulation results were provided to demonstrate the effectiveness of our

proposed solution. For our future work, the extension to consider mobile UAV with trajectory design and short-packet offloading will be further studied.

## REFERENCES

- [1] N. Deng et al., "Enhancing Millimeter Wave Cellular Networks via UAV-Borne Aerial IRS Swarms," *IEEE Trans. Commun.*, vol. 72, no. 1, pp. 524-538, Jan. 2024.
- [2] Y. Zhou et al., "Secure Multi-Layer MEC Systems With UAV-Enabled Reconfigurable Intelligent Surface Against Full-Duplex Eavesdropper," *IEEE Trans. Commun.*, vol. 72, no. 3, pp. 1565-1577, March 2024.
- [3] Q. Wu, Y. Zeng, and R. Zhang, "Joint Trajectory and Communication Design for Multi-UAV Enabled Wireless Networks," *IEEE Trans. Wireless Commun.*, vol. 17, no. 3, pp. 2109-2121, March 2018.
- [4] X. Shi and N. Deng, "Modeling and Analysis of mmWave UAV Swarm Networks: A Stochastic Geometry Approach," *IEEE Trans. Wireless Commun.*, vol. 21, no. 11, pp. 9447-9459, Nov. 2022.
- [5] Z. Zhang et al., "6G Wireless Networks: Vision, Requirements, Architecture, and Key Technologies," *IEEE Vehicular Technology Magazine*, vol. 14, no. 3, pp. 28-41, Sept. 2019.
- [6] D. Wang et al., "Task Offloading and Trajectory Scheduling for UAV-Enabled MEC Networks: An Optimal Transport Theory Perspective," *IEEE Wireless Commun. Lett.*, vol. 11, no. 1, pp. 150-154, Jan. 2022.
- [7] F. Pervez, A. Sultana, C. Yang, and L. Zhao, "Energy and Latency Efficient Joint Communication and Computation Optimization in a Multi-UAV-Assisted MEC Network," *IEEE Trans. Wireless Commun.*, vol. 23, no. 3, pp. 1728-1741, March 2024.
- [8] Y. Liu, S. Xie, and Y. Zhang, "Cooperative Offloading and Resource Management for UAV-Enabled Mobile Edge Computing in Power IoT System," in *IEEE Trans. Veh. Technol.*, vol. 69, no. 10, pp. 12229-12239, Oct. 2020.
- [9] J. Chen et al., "Deep Reinforcement Learning Based Resource Allocation in Multi-UAV-Aided MEC Networks," *IEEE Trans. Commun.*, vol. 71, no. 1, pp. 296-309, Jan. 2023.
- [10] Y. Huang, Y. Hu, X. Yuan and, A. Schmeink, "Analytical Optimal Joint Resource Allocation and Continuous Trajectory Design for UAV-Assisted Covert Communications," *IEEE Transactions on Wireless Communications*, vol. 24, no. 1, pp. 213-227, Jan. 2025.
- [11] X. Chen et al., "Covert Communications: A Comprehensive Survey," in *IEEE Commun. Surv. Tutor.*, vol. 25, no. 2, pp. 1173-1198, Secondquarter 2023.
- [12] X. Zhou et al., "Joint Optimization of a UAV's Trajectory and Transmit Power for Covert Communications," in *IEEE Trans. Signal Process.*, vol. 67, no. 16, pp. 4276-4290, 15 Aug. 2019.
- [13] X. Jiang, Z. Yang, N. Zhao, Y. Chen, Z. Ding, and X. Wang, "Resource Allocation and Trajectory Optimization for UAV-Enabled Multi-User Covert Communications," in *IEEE Trans. Veh. Technol.*, vol. 70, no. 2, pp. 1989-1994, Feb. 2021.
- [14] X. Zhou, S. Yan, D. W. K. Ng and R. Schober, "Three-Dimensional Placement and Transmit Power Design for UAV Covert Communications," in *IEEE Trans. Veh. Technol.*, vol. 70, no. 12, pp. 13424-13429, Dec. 2021.
- [15] Y. Zhou et al., "Energy-Efficient Covert Communications for UAV-Assisted Backscatter Systems," accepted in *IEEE Trans. Veh. Technol.*, 2024, doi: 10.1109/TVT.2024.3359182.
- [16] X. Chen et al., "UAV-IRS Assisted Covert Communication: Introducing Uncertainty via Phase Shifting," *IEEE Wireless Commun. Lett.*, vol. 13, no. 1, pp. 103-107, Jan. 2024.
- [17] Y. Zhou, Y. Wang, Z. Ma, P. Fan and M. Xiao, "Physical Layer Authentication for UAV Communications Under Rayleigh and Rician Channels," in *IEEE Transactions on Wireless Communications*, vol. 24, no. 4, pp. 2722-2733, April 2025.
- [18] C. Xu, C. Zhan, H. Yang and L. Xiao, "Pareto-Optimal Aerial-Ground Energy Minimization for Aerial 3D Mobile Edge Computing Networks," in *IEEE Transactions on Vehicular Technology*, vol. 73, no. 5, pp. 7218-7233, May 2024.
- [19] Q. Luo et al., "Minimizing the Delay and Cost of Computation Offloading for Vehicular Edge Computing," in *IEEE Transactions on Services Computing*, vol. 15, no. 5, pp. 2897-2909, 1 Sept.-Oct. 2022.
- [20] W. Wang, W. Ni, H. Tian, and L. Song, "Intelligent Omni-Surface Enhanced Aerial Secure Offloading," *IEEE Trans. Veh. Technol.*, vol. 71, no. 5, pp. 5007-5022, May 2022.